Replication protein-A, RPA, plays a pivotal role in the maintenance of recombination checkpoint in yeast meiosis

Arivarasan Sampathkumar, Zhong Chen, Yuting Tang, Yurika Fujita, Masaru Ito, and Akira Shinohara*

Institute for Protein Research, Osaka University, Suita, Osaka 565-0871, Japan

Running title: Essential role of RPA in recombination checkpoint

Keywords: meiosis; homologous recombination; RPA; recombination checkpoint; Rfa1, auxin degron, synapsis checkpoint

*Corresponding author:
Akira Shinohara; ashino@protein.osaka-u.ac.jp

Lead contact:
Akira Shinohara
Institute for Protein Research, Osaka University,
3-2 Yamadaoka, Suita, Osaka 565-0871 JAPAN
Phone: 81-6-6879-8624
FAX: 81-6-6879-8626
E-mail: ashino@protein.osaka-u.ac.jp
ORCID: 0000-0003-4207-8247

Summary

DNA double-strand breaks (DSBs) activate DNA damage responses (DDR) in both mitotic and meiotic cells. A single-stranded DNA (ssDNA) binding protein, Replication protein-A (RPA) binds to the ssDNA formed at DSBs to activate ATR/Mec1 kinase for the response. Meiotic DSBs induce homologous recombination monitored by a meiotic DDR called the recombination checkpoint that blocks the pachytene exit in meiotic prophase I. In this study, we showed the essential role of RPA in the maintenance of the recombination checkpoint during *S. cerevisiae* meiosis. The depletion of an RPA subunit, Rfa1, in a recombination-defective *dmc1* mutant, fully alleviates the pachytene arrest with the persistent unrepaired DSBs. RPA depletion decreases the activity of a meiosis-specific CHK2 homolog, Mek1 kinase, which in turn activates the Ndt80 transcriptional regulator for pachytene exit. These support the idea that RPA is a sensor of ssDNAs for the activation of meiotic DDR. Rfa1 depletion also accelerates the prophase I delay in the *zip1* mutant defective in both chromosome synapsis and the recombination, suggesting that the accumulation of ssDNAs rather than defective synapsis triggers prophase I delay in the *zip1* mutant.

Introduction

A eukaryotic single-stranded (ss)DNA binding protein, Replication protein-A (RPA), plays an essential role in DNA replication, DNA repair, and homologous recombination [1-3]. RPA consists of three subunits; RPA70(RPA1), RPA32(RPA2), and RPA14(RPA3), which are highly conserved from yeast to humans. In *S. cerevisiae*, the knockout of either one of three genes (*RFA1*, *-2* and *-3*) encoding the RPA subunits leads to lethality, consistent with its essential role in DNA replication [4]. RPA also plays a role in DNA damage response (DDR) [3,5].

In homologous recombination. RPA binds to ssDNAs to prevent the formation of the secondary structure of ssDNAs and to protect ssDNAs from degradation by various nucleases [6]. The assembly of Rad51 filaments on RPA-coated ssDNA is assisted by Rad51 mediators such as Rad52 in the budding yeast [7-9]. RPA assists Rad51-mediated homology search and strand exchange with a homologous double-stranded (ds)DNA [10]. The invasion of the ssDNA into the homologous dsDNA results in the formation of a displacement loop (D-loop). The 3'-OH end of the invading strand provides a substrate for DNA synthesis, which is followed by further processing and engaging with the ssDNA in the other DSB end to form a joint molecule. The joint molecule is finally matured into a

recombination product. RPA also works in recombination-associated DNA synthesis as well as the annealing in the second-end capture.

DNA double-strand break (DSB) activates the DDR. DSB ends stimulate a DDR kinase, ATM/Tel1 (Ataxia telangiectasia mutated) while ssDNAs do an ATM homolog, ATR/Mec1 (Ataxia telangiectasia mutated related), both of which belong to the PI3 kinase family [11,12]. The activation of ATR is mediated by the interaction with an ATR partner, ATRIP/Ddc2, which directly interacts with RPA bound to ssDNAs [13-15]. In mammals, ATR activation is also mediated by the second RPA-binding protein, ETAA1 [16,17]. Thus, RPA is considered to work as an essential DNA damage sensor to ssDNAs as well as a DNA damage processing protein.

Meiosis rewires DNA transactions such as homologous recombination/DSB repair as well as DDR to guarantee the faithful segregation of two paternal homologous chromosomes at meiosis I for the reduction of chromosome numbers in gametes. In budding yeast, meiotic recombination is initiated by the DSB formation at recombination hotspots by the TopoVI-like protein, Spo11, which is followed by the production of ssDNAs [18,19]. The ssDNA is used by a meiosis-specific Rad51 homolog, Dmc1 [20], for D-loop formation, which is aided by Rad51 [21] and its mediator, Mei5-Sae3 complex [22,23]. Further processing generates a recombination intermediate with double-Holliday junctions (dHJs), which are specifically resolved into crossovers between homologs. Importantly, the partner choice in the recombination is mediated by meiosis-specific chromosome-axis proteins (Hop1, Red1, and Mek1/Mre4), promoting interhomolog bias via an unknown mechanism [24-26]. Mek1/Mre4 (hereafter Mek1), a meiosis-specific homolog of Rad53/CHK2 kinase [27,28], suppresses Rad51-mediated recombination in meiosis [25,26]. This suppression occurs through the Mek1-mediated phosphorylation of two proteins, Rad54 and Hed1 [29,30]. Rad54 belongs to the Swi2/Snf2 family protein essential for Rad51-mediated strand invasion [31]. Mek1-mediated phosphorylation of Rad54 abolishes its interaction with Rad51 [30]. Hed1, which is expressed only in meiosis, inhibits Rad51 by binding to the Rad51-ssDNA complex [32]. The inhibitory activity of Hed1 against Rad51 and the stability of Hed1 are augmented by the Mek1-mediated phosphorylation [29].

Meiotic events such as recombination and chromosome synapsis are strictly coupled with each other (Fig. 1) [33]. Similar to mitosis, DSBs in yeast meiosis activate Tel1(ATM) and Mec1(ATR). Different from mitotic DNA damage

100 checkpoint, downstream events of Mec1 or Tel1 activation such as the Rad53
101 activation are largely suppressed in meiotic cells with poorly-defined mechanisms
102 [34,35]. On the other hand, Mec1 and/or Tel1 phosphorylates Hop1 on chromosome
103 axis [36]. Together with chromosomal-bound Red1, phosphorylated Hop1 activates
104 Mek1 kinase, whose autophosphorylation provides positive feedback on its
105 activity [37]. Mek1-mediated phosphorylation promotes the inactivation of the Ndt80
106 transcription factor [38] essential for the exit from the pachytene stage, where
107 chromosome synapsis and the formation of the dHJs are completed [37,39]. By
108 activating Ndt80 (through inactivating Mek1), meiotic cells exit the pachytene
109 stage by expressing downstream targets such as Cdc5 Polo-like kinase (PLK)
110 and a cyclin, Clb1 [40] for the resolution of dHJs and the disassembly of the
111 synaptonemal complex (SC), a meiosis-specific tripartite chromosome structure,
112 an indicative of chromosome synapsis.
113 It is widely accepted that meiotic cells surveil not only homologous
114 recombination but also chromosome synapsis, referred to as the “recombination”
115 and “synapsis” checkpoints (Fig. 1). Like a recombination-defective *dmc1* mutant,
116 the budding yeast *zip1* mutant, which is defective in the assembly of the central
117 region of the SCs, thus synapsis shows a delay in meiosis progression [41]. In
118 nematodes and mice, synapsis-defective mutants also delay the meiotic
119 prophase I progression and/or induce apoptosis [42,43]. In yeast, chromosome
120 synapsis is tightly coupled with meiotic recombination: e.g. a recombination-
121 deficient mutant also displays abnormal synapsis [44,45]; the *zip1* mutant completely
122 defective in SC formation also impairs the processing of meiotic recombination
123 intermediates. This complicates the presence of the synapsis checkpoint.
124 Moreover, DDR proteins also play a role in meiotic recombination, which also
125 provides a caveat in the interpretation of the meiotic phenotypes of DDR mutants
126 [46-48].
127 The role of RPA in DDR is widely accepted. In a pioneer work [5], the depletion
128 of RPA70 in human cell lines reduced the ATRIP/Ddc2 binding to the DNA
129 damage as well as the activation of downstream events. In the same study, it was
130 also shown that the depletion of Rfa1 in mitotic yeast cells by a temperature-
131 induced degron reduced the binding of Ddc2 to a single DSB. On the other hand,
132 the other report showed that Rfa1 depletion in G2/M-arrested mitotic cells in
133 budding yeast by the degron does not affect checkpoint activation to a single DSB
134 [6]. A point mutant in the *RFA1* gene encoding RPA70 subunit of yeast RPA called
135 *rfa1-t11* with K45E substitution in the N-terminal protein-protein interaction

136 domain is partially defective in the DDR in the response to telomere dysfunction
137 [49]. Rfa1-t11 showed normal binding to the DSB, but the mutant decreased
138 recruitment of Ddc2 to the DSB [5]. In meiosis, the *rfa1-t11* with reduced Ddd2-
139 focus formation in nuclei weakly suppresses the *dmc1*-induced delay in meiosis
140 progression [50] while RPA containing Rfa1-t11 showed normal localization on
141 meiotic chromosomes [51]. The *rfa1-t11* mutant alters recombination kinetics [51],
142 which may indirectly affect the checkpoint. Furthermore, the conditional depletion
143 of Rpa1 in mouse spermatocytes eliminated RPA foci on meiotic chromosomes
144 but is proficient in ATR recruitment to the chromosomes [52]. Therefore, we still
145 need careful evaluation of the role of RPA in the DDR in meiotic cells.
146 In this study, we revisited the role of RPA in the meiotic recombination
147 checkpoint by using a conditional-depletion mutant of Rfa1. The depletion of Rfa1
148 in the *dmc1*-induced pachytene arrest facilitates the pachytene exit, thus entry
149 into meiosis I and II. Importantly, the RPA depletion did not change the
150 accumulation unrepaired meiotic DSBs in the *dmc1*, which causes abnormal
151 segregation of chromosomes in the division. This confirms the essential role of
152 RPA in the maintenance of the meiotic recombination checkpoint. Moreover, we
153 found that Rfa1 depletion also alleviates delayed meiosis progression in the *zip1*
154 mutant. This suggests that the *zip1* mutation mainly triggers an RPA-dependent
155 response of the prophase I delay, thus the recombination checkpoint rather than
156 the synapsis checkpoint.
157
158 **Results**
159 **Depletion of Rfa1 alleviates *dmc1*-induced arrest of meiosis**
160 Three RPA subunits, Rfa1, -2, and -3, are essential for the viability of budding
161 yeast cells [4]. To know the role of RPA in the DDR in yeast meiosis, we constructed
162 a conditional depletion mutant of the *RFA1* gene encoding the largest RPA
163 subunit, Rfa1, by the auxin-induced degron (AID) system [53]. The AID tag was
164 added to the C-terminal of the Rfa1 protein. The addition of auxin as well as
165 copper, which induced Tir1 F-box protein, in the medium largely inhibited the
166 mitotic growth of *RFA1-AID* cells (Supplemental Fig. 1a), consistent with the
167 previous study [4]. *RFA1-AID* diploid cells were induced for the entry of meiosis by
168 incubating in the sporulation medium (SPM). When auxin was added at 4 h
169 incubation with SPM after pre-meiotic DNA replication, which induced the
170 disappearance of Rfa1 from 5 h (Supplemental Fig. 1b), the cells formed few
171 spores after 24 h while more than 90% of the control wild-type cells sporulated

172 (Supplemental Fig. 1c). Most of the Rfa1-depleted cells showed abnormal
173 nuclear morphology (Supplemental Fig. 1c). Indeed, rarely formed tetrad of the
174 cells are all dead (0 viable spores in 100 tetrads) while without the auxin treatment,
175 the viability of spores from *RFA1-AID* cells was 91.8% (among 100 tetrads). The
176 pulse-field gel electrophoresis revealed the accumulation of meiotic DSBs on
177 chromosomes (Supplemental Fig. 1d), confirming a defect in DSB repair [51].
178 These show that the AID-tag did not interfere with Rfa1 function in both miotic
179 and meiotic cells and that Rfa1 is essential for both mitosis and meiosis.
180 To know the role of RPA in the recombination checkpoint in meiosis, we
181 used the *dmc1* mutant, which is unable to repair meiotic DSBs and, as a result,
182 shows an arrest at mid-pachytene stage during meiotic prophase I [20]. This
183 response to unrepaired DSBs is referred to as the recombination checkpoint.
184 *RFA1-AID* was introduced in the *dmc1* deletion mutant; *dmc1 RFA1-AID*. Like the
185 *dmc1* mutant, without auxin addition, *dmc1 RFA1-AID* shows an arrest in meiotic
186 prophase I without division (e.g. Fig. 2d), indicating that the Rfa1 tagging did not
187 affect the recombination checkpoint in the absence of Dmc1. RPA is also involved
188 in DNA replication and S-phase checkpoint [1,2], which indirectly affects the G2
189 event. To avoid the effect in pre-meiotic DNA replication, we depleted Rfa1 protein
190 by adding auxin to a meiotic culture of *dmc1 RFA1-AID* cells at 4 h after the
191 induction of meiosis in the sporulation medium (SPM), thus, after pre-meiotic DNA
192 replication, which occurs at 1.5-3 h. At 5 h, after the 1-hour addition of auxin, the
193 protein level of Rfa1-AID was decreased to ~15% level relative to the original
194 level at 4 h (Fig. 2a, Supplementary Figs. S1e and S2), indicating the efficient
195 depletion of Rfa1 under the condition. We also checked the focus formation of
196 Rfa2, the second subunit of RPA, on meiotic chromosome spreads. Rfa2 shows
197 punctate staining on the spreads with other recombination proteins such as
198 Rad51 [54], which corresponds with ongoing recombination (Fig. 2b). In the *dmc1*
199 mutant, Rfa2 focus-staining appears at 2.5 h, reaches a plateau at 5 h, and
200 persists after that, indicating little turnover of Rfa2 due to stalled recombination in
201 the mutant (Fig. 2c, Supplementary Fig. S3a). When auxin was added at 4 h,
202 Rfa2 foci disappeared within one hour, and Rfa2 foci were rarely observed during
203 further incubation by 10 h (Fig. 2b, c). This suggests that RPA is highly dynamic
204 and easily dissociated from the chromosome. We concluded that Rfa1 depletion
205 at 4 h in meiosis eliminates most chromosome-bound RPA complexes by 5 h.
206
207 **Checkpoint alleviation in Rfa1 depletion in *dmc1* meiosis**

208 DAPI staining of DNAs confirmed a single DAPI body in a *dmc1 RFA1-AID* cell
209 even at 24 h, thus an arrest in prophase I as shown previously [20]. Rfa1 depletion
210 at 4 h induced fragmentation of DAPI bodies at late time points. In some cells, 2-
211 4 irregular-sized DAPI bodies with smaller DAPI bodies were detected in a single
212 cell (Fig. 2d). The cells with abnormal DAPI bodies appeared at 6 h and gradually
213 accumulated by 24 h (Fig. 2e). This suggests the presence of nuclear division,
214 thus the onset of meiosis I and/or II in the *dmc1* cells upon Rfa1 depletion. We
215 also checked the effect of Rfa1 depletion on meiotic DNA replication. The FACS
216 analysis showed that the addition of auxin at 4 h did not affect the transition from
217 2C to 4C (Supplementary Fig. S1f).
218 To evaluate the meiosis progression precisely, we examined the status of
219 spindle morphology in the *dmc1 RFA1-AID* cells in the absence or presence of
220 auxin (Fig. 2f, g). Tubulin staining revealed a single focus associated with single
221 or multiple short projections in meiotic prophase I of the cell in the absence of
222 auxin (Fig. 2f). The *dmc1 RFA1-AID* mutant maintained this arrangement of
223 spindles in the absence of auxin by 24 h, consistent with an arrest of the *dmc1*
224 mutant in prophase I (Fig. 2f). On the other hand, the Rfa1 depletion induced the
225 elongation of spindles after one hour of addition (at 5 h). At 6 h, ~50% *dmc1*
226 *RFA1-AID* cells contained single short and long spindles corresponding with
227 metaphase I and anaphase I, respectively (Fig. 2e). At 8 h, in addition to the
228 metaphase I and anaphase I spindle, ~70% of cells contained metaphase II or
229 anaphase II spindles (Fig. 2f, g). At 10 h, most of the cells showed diffuse staining
230 of microtubules in multiple DAPI bodies in a cell. These show that Rfa1 depletion
231 almost alleviates meiotic prophase I arrest induced by the *dmc1* mutation.
232 Cdc5/PLK is expressed after the pachytene exit [40,55]. Like *dmc1* cells,
233 without auxin addition, the *dmc1 RFA1-AID* mutant cells did not express Cdc5
234 (Fig. 2a). On the other hand, the addition of auxin at 4 h induced the expression
235 of Cdc5 from 5 h. This confirms the exit of the pachytene stage of *dmc1* cells in
236 the absence of RPA.
237
238 **No DSB repair in *dmc1* meiosis with Rfa1 depletion**
239 One possibility to suppress the *dmc1* arrest is to channel unrepaired DSBs into
240 the repair pathway. On the other hand, the acute depletion of RPA did not affect
241 the status of meiotic DSBs under *dmc1* arrest. The CHEF (Counter-clamped
242 homogeneous electric field) gel electrophoresis confirmed the accumulation of
243 fragmented chromosomes in the *dmc1* mutant irrespective of the presence or

244 absence of RPA. In the *dmc1 RFA1-AID* mutant without auxin treatment, smear
245 bands of full-length chromosomes appeared at 3 h and most of the chromosomes
246 became fragmented with a size of less than 700 kbp by 5 h. After 6 h, fragmented
247 chromosomes persisted by 24 h (Fig. 3a, Supplementary Fig. S4 for wild-type
248 control). The depletion of Rfa1 from 4 h did not affect the persistence of
249 fragmented chromosomes. This suggests that meiotic DSBs remain unrepaired
250 under the depletion of RPA in the *dmc1* mutant.
251 We also indirectly checked the DSB status by analyzing Rad51 foci on
252 meiotic chromosomes (Fig. 3b, c). Like Rfa2 foci, in the *dmc1 RFA1-AID* mutant
253 in the absence of auxin, Rad51 foci appeared at 4 h, reached a plateau at 5 h,
254 and persisted at late times as shown previously [56]. The addition of auxin at 4 h
255 rapidly induced the disappearance of Rad51 foci at 5 h. The reduced Rad51 foci
256 are seen at late time points (Fig. 3c and Supplementary Fig. 3b). This suggests
257 that RPA is critical for the maintenance of Rad51 foci on the chromosomes. The
258 absence of Rad51 foci in the Rfa1 depletion supports the inability of *dmc1 RFA1-*
259 *AID* cells without RPA to repair meiotic DSBs by Rad51-dependent recombination.
260
261 **The Hop1/Mek1-Ndt80 axis was down-regulated after RFA1 depletion**
262 Un-repaired DSBs in the *dmc1* mutant activate the recombination checkpoint,
263 which down-regulates a meiosis-specific transcription activator, Ndt80 for the
264 pachytene exit (Fig. 1). DSB-activated Mec1/ATR kinase phosphorylates a
265 HORMAD protein, Hop1, which stimulates a meiosis-specific kinase, Mek1. Mek1
266 binds and phosphorylates Ndt80 to inactivate it. For pachytene exit, further
267 phosphorylation of Nd80 by Ime2 kinase promotes the activation of Ndt80 [38]. In
268 *dmc1 RFA1-AID* cells, the Ndt80 appeared at 4 h with multiple bands and
269 accumulated more during further incubation in SPM without a change of band-
270 shift status (Fig. 2a). At 6 h, after two hours of addition of auxin, a slower-
271 migrating Ndt80 band appeared and accumulated. Importantly, as shown above,
272 under the depletion condition, Cdc5/PLK, which is a major target of activated
273 Ndt80 and is necessary for pachytene exit, appeared at 6 h (Fig. 2a). This is
274 consistent with meiosis progression of the *dmc1* mutant cells induced by Rfa1-
275 depletion.
276 We also checked the behavior of the upstream regulators of Ndt80, and
277 Hop1 by western blotting. In the *dmc1* mutant, Hop1 appeared as a non-
278 phosphorylated form at 2 h and phosphorylated Hop1 with slower migrated bands
279 persisted from 4 h (Fig. 2a) as shown previously [36]. After Rfa1 depletion, major

280 bands of phosphorylated Hop1 almost disappeared from 6 h with a similar steady-
281 state level of non-phosphorylated Hop1 during the time course. This suggests
282 that Hop1 is de-phosphorylated during pachytene exit. On chromosome spreads,
283 Hop1 shows beads-in-line staining for the localization of chromosome axes (Fig.
284 3d) [57,58]. In the *dmc1* mutant without Rfa1 depletion, Hop1 localization remains
285 unchanged during meiosis (Fig. 3d). The addition of auxin at 4 h induced the
286 disappearance of Hop1-positive spreads from 5 h. At 6 h, ~35% of cells are
287 positive for Hop1 while ~95% are positive in a control (Fig. 3d, e). At 8 h, most of
288 the Hop1 signals on the chromosomes disappeared.
289 One of the Mek1 kinase targets is histone H3T11 phosphorylation [59]. Under
290 the *dmc1* arrest condition, H3T11 phosphorylation accumulated (Fig. 2a). On the
291 other hand, the Rfa1 depletion rapidly induced the disappearance of the signal
292 (Fig. 2a), suggesting the downregulation of Mek1 activity under Rfa1 depletion.
293 These results clearly showed that Rfa1, thus RPA, is critical for the maintenance
294 of the recombination checkpoint through the Hop1/Mek1-Ndt80 axis.
295 The *dmc1*-induced arrest in meiosis is also partially suppressed by the
296 *rad51* [60]. A recent study showed that the suppression of *dmc1*-arrest by the *rad51*
297 mutation is mediated by partial elongation of SCs with concomitant loss of Hop1
298 [61]. Rad51 loss from the chromosomes in the *dmc1* mutant upon Rfa1-depletion
299 such as 5-h time point by 4-h addition of auxin seems to mimic a condition seen
300 in the *rad51 dmc1* double mutant. To address whether Rad51-focus loss in the
301 *dmc1* mutant by Rfa1 depletion induced SC formation, we checked SC formation
302 by staining Zip1, a component of SC central region [41]. The Zip1 staining is
303 classified into three classes; dots, short lines, and long lines. As shown previously
304 [20], the *dmc1* mutant is defective in SC elongation (Supplemental Fig. 5a, b). Rfa1
305 depletion promotes the SC disassembly by the pachytene exit. At 5 h when most
306 of Rad51 foci disappeared, we did not see elongation of Zip1 lines relative to
307 control with Rad51 foci and rather observed increased Zip1 polycomplex, which
308 is indicative of defective SC assembly (Supplemental Fig. 5c). Moreover, Hop1
309 localization one-hour after Rfa1 depletion is similar to that without the depletion
310 (Fig. 3d, e). These suggests that the suppression of arrest by Rfa1 depletion is
311 unlikely to come from altered Hop1 functions as seen in the *rad51 dmc1* double
312 mutant [61].
313
314 **Bypass of *dmc1* arrest by Rfa1 depletion depends on Ndt80**
315 We tested whether the pachytene exit of the *dmc1* cells by Rfa1 depletion

316 depends on the *NDT80* (Fig. 4). The addition of auxin to *dmc1 ndt80 RFA1-AID*
317 cells efficiently reduced the amount of Rfa1 protein (Fig. 4a, Supplementary Fig.
318 S6) and Rfa2 foci from meiotic chromosomes (Fig. 4b). However, different from
319 the *dmc1 RFA1-AID* mutant, the addition of auxin to *dmc1 ndt80 RFA1-AID*
320 mutant did not induce the elongation of spindles (Fig. 4c) or Hop1 disassembly
321 from the chromosomes (Fig. 4d). Thus, the pachytene exit of *dmc1* cells by Rfa1
322 depletion still depends on Ndt80. Interestingly, the amount of the phosphorylated
323 Hop1 is reduced slightly compared to that in the control (Fig. 4a). This is less
324 drastic compared to the presence of Ndt80, supporting an auto-feedback
325 mechanism between Mek1 activation and Ndt80 activation [62].
326
327 **Checkpoint alleviation in Rfa1 depletion in *zip1* meiosis**
328 Meiotic yeast cells monitor not only ongoing meiotic recombination but also
329 chromosome synapsis [43]. However, the presence of the so-called "synapsis
330 checkpoint" in yeast meiosis is under debate [62]. The mutant in the *ZIP1* gene is
331 deficient in chromosome synapsis with a delay of the entry into meiosis I and is
332 used to analyze the synaptic checkpoint [41]. We examined the effect of Rfa1
333 depletion on the *zip1*-induced delay of meiosis I (Fig. 5). As reported previously
334 [45], in the SK1 strain background, *zip1 RFA1-AID* cells without auxin addition
335 started meiosis I at 8 h while wild-type cells entered at 5 h (and finished meiosis
336 II by 10 h) (Fig. 5b). When auxin was added at 4 h, which induced rapid depletion
337 of Rfa1 and the dissociation of Rfa2 from meiotic chromosomes (Fig. 5a, c, h,
338 Supplementary Fig. S7), metaphase I spindles appeared at 5 h, and at 6 h, ~35%
339 of the cells contained metaphase-I and anaphase-I spindles (Fig. 5d, e). At 8 h,
340 ~30% of the cells contained anaphase-II spindle. Importantly, DAPI staining
341 showed the entry of the *zip1* cells into meiosis I upon Rfa1 depletion is similar to
342 that in wild-type cells (Fig. 5b). The spore viability of *zip1 RFA1-AID* cells treated
343 with auxin was 0% while cells without auxin was 35.5% (among 100 tetrads).
344 The *zip1 RFA1-AID* cells without auxin expressed Cdc5 from 8 h (Fig. 5a),
345 consistent with delayed progression of prophase I in the mutant. The addition of
346 auxin at 4 h accelerated the Cdc5 expression from 5 h. The *zip1* mutant
347 accumulated H3T11 phosphorylation of histone H3 signal from 4 h to 8 h (Fig.
348 5a). The Rfa1 depletion accelerated the disappearance of this phosphorylation
349 from 5 h. The accelerated disappearance of the phospho-Hop1 protein is also
350 seen by the depletion (Fig. 5a, f). These showed the Rfa1-dependent inactivation
351 of the Hop1/Mek1-Ndt80 signaling pathway induced by the *zip1* mutation. Thus,

352 the delay induced by the *zip1* mutation largely depends on the Rfa1.
353 In addition to SC formation, Zip1 plays a critical role in meiotic recombination
354 as a pro-crossover factor. Indeed, the *zip1* mutant shows delayed DSB repair.
355 The CHEF analysis showed the presence of broken chromosomes in the *zip1*
356 mutant from 3 h to 7 h (Fig. 5g). Importantly, full-length chromosomes were
357 reassembled at 10 h without Rfa1 depletion, indicating that most of the DSBs in
358 the *zip1* mutant were repaired with the delay. On the other hand, Rfa1 depletion
359 from 4 h induced fragmentation of the chromosomes from 5 h. Even after 24 h,
360 little recovery of full-length chromosomes was seen under the condition. This
361 suggests that Rfa1 is essential for meiotic DSB repair in the *zip1* mutant.
362
363 **Rfa1 depletion does not alleviate delay induced by *rad50S* meiosis**
364 The *rad50S* mutant, which is defective in the end-processing of meiotic DSBs,
365 also shows delayed meiosis I progression [63]. This delay in the *rad50S* mutant is
366 mediated by Tel1(ATM) and Rad50-Mre11-Xrs2, which recognize DSB ends [64].
367 The pathway is distinct from the Mec1(ATR)-mediated pathway shown above. We
368 also examined the effect of Rfa1 depletion on the *rad50S*-induced delay (Fig. 6a,
369 Supplementary Fig. S8). As reported, without auxin, *rad50S RFA1-AID* cells delay
370 the onset of meiosis I as shown by whole-cell staining of tubulin (Fig. 6b). Rather,
371 the addition of auxin to the *rad50S RFA1-AID* cells delayed the onset of meiosis
372 I more than without the auxin. We cannot detect Rfa2 foci in the r*ad50S* mutant
373 even in the presence of Rfa1 (Fig. 6c), confirming that the *rad50S* accumulates
374 unresected DSBs [63]. Moreover, Hop1 phosphorylation is not observed in the
375 mutant (Fig. 6a). This is consistent with little formation of ssDNAs without DSB
376 processing in the mutant [63], thus little Mec1/ATR activation. This is expected since
377 the *rad50S* mutant does not form any ssDNAs, which is a substrate for RPA. The
378 accumulation of chromosomal Hop1 in the mutant is not affected by the Rfa1
379 depletion (Fig. 6d).
380
381 **Discussion**
382 RPA plays multiple roles in DNA replication, DNA repair, and recombination
383 through its ability to bind to ssDNAs with a high affinity. RPA is also important for
384 DDR as a sensor of DNA damage, thus ssDNAs. The role of RPA in Mec1(ATR)
385 activation through the binding of Mec1(ATR)-interaction protein, Ddc2(ATRIP), to
386 RPA has been documented well [5,13,14]. In this paper, we showed the pivotal role
387 of RPA in the maintenance of DDR in meiosis, called recombination checkpoint.

388

389 **The role of RPA in recombination checkpoint**

390 Previously, in the budding yeast, two *RFA1*-degron mutants, *rfa1-td* and *td-RFA1*,
391 were constructed and characterized to study the role of Rfa1 in DDR activation.
392 Indeed, the *rfa1-td*, as well as the *rft1-t11 (rfa1-K45E)* mutant, reduce the
393 recruitments of Ddc2 to a DSB site [5]. On the other hand, it is shown that, by using
394 the *td-RFA1*, G2/M-arrested haploid cells depleted for Rfa1 still activate Rad53
395 upon a single DSB [6]. The latter study concludes that a low level of RPA is
396 sufficient for the activation of Mec1-Ddc2. More recently, an RPA-independent
397 pathway for ATR activation, which requires APE1, was identified in *Xenopus* egg
398 extracts [65]. We revisited the role of RPA in DDR by studying the effect of Rfa1
399 depletion in DDR such as the meiotic recombination checkpoint. The
400 recombination checkpoint in meiotic cells responds to the ssDNA through RPA-
401 Mec1-Ddc2 axis as seen in a canonical DNA damage checkpoint in mitotic cells.
402 By using the auxin-degron, we depleted Rfa1 in the *dmc1* mutant which arrests
403 in meiotic prophase I with hyper-resected ssDNAs in ~150 DSBs [20]. The Rfa1-
404 depletion induced the pachytene exit by downregulating Mec1 and Mek1
405 activities, which in turn activates the Ndt80-dependent gene expression of key
406 regulators for the pachytene exit such as Cdc5 [40,55]. This is consistent with the
407 previous study which showed that the *rfa1-t11* with reduced Ddd2-focus formation
408 in nuclei weakly suppresses the *dmc1*-induced delay [50]. Importantly, the Rfa1
409 depletion did not affect the accumulation of ssDNAs in the *dmc1* cells with
410 persistent unrepaired DSBs. This is particularly important since mutations in DDR
411 genes such as *RAD17*, *-24*, *DDC1*, and *MEC3* even in the *MEC1* gene bypass
412 the *dmc1*-induced arrest by repairing DSBs by an alternative pathway such as
413 ectopic recombination [46,48,66]. The results described here supported the idea that
414 RPA is a sensor for ssDNAs, which creates a scaffold for the assembly of
415 checkpoint effectors such as Mec1-Ddc2(ATR-ATRIP). In meiosis, meiosis-
416 specific Mek1 is activated through the phosphorylation of Hop1 by Mec1 kinase
417 [36]. The Rfa1-depletion induces rapid dephosphorylation of Hop1 and the
418 dissociation from meiotic chromosomes without affecting the protein level,
419 suggesting the presence of an active de-phosphorylation pathway of Hop1.

420

421 **The chromosome synapsis checkpoint in yeast meiosis**

422 In addition to the recombination checkpoint, meiotic cells responds to abnormal
423 chromosome synapsis, which is called synapsis checkpoint. This idea was

424 proposed that mutants defective in chromosome synapsis show a delay in the
425 progression of prophase I and apoptosis in yeasts and mice or nematodes,
426 respectively. However, the presence of the synapsis checkpoint is still under
427 debate [42,43], since in most organisms meiotic recombination and chromosome
428 synapsis are tightly coupled. The budding yeast *zip1* mutant, which is completely
429 defective in SC formation, thus, chromosome synapsis, delays or arrest in meiotic
430 prophase I [41,45]. This arrest is alleviated by the mutant of genes encoding a
431 component of checkpoint such as *PCH2* [67]. Pch2 modulates Hop1 conformation
432 and regulates the association and dissociation of Hop1 on meiotic chromosomes
433 [61,68,69]. On the other hand, the *zip1* mutant also shows defective DSB repair
434 and/or the crossing-over [44,45], which suggests delayed progression of meiosis I in
435 the *zip1* mutant is caused by the impaired recombination. In this study, by using
436 the *RFA1-AID*, we could test whether the delay in *zip1* mutant depends on RPA
437 or not and found that the Rfa1-depletion eliminates the delay induced by the *zip1*
438 mutation. This strongly suggests that the recombination checkpoint delays the
439 meiosis I progression in the *zip1* mutant as seen in the *dmc1* mutant. Moreover,
440 consistent with this, the other yeast mutants, which are fully defective in the
441 synapsis with a weak recombination defect such as *ecm11* and *gmc2*, do not
442 show a drastic delay in the meiosis I progression [70,71]. Thus, at least in budding
443 yeast which couples the recombination and chromosome synapsis, rather than
444 the status of chromosome synapsis, a recombination process, the presence of
445 ssDNAs, can be monitored by a meiosis-specific surveillance mechanism to
446 guarantee the completion of meiotic recombination directly and chromosome
447 synapsis indirectly. Our idea is consistent with the idea proposed by recent
448 reports claiming the merging of the recombination and synapsis checkpoints in
449 meiosis [61,72].
450
451 **Methods**
452 **Strains and plasmids**
453 All strains described here are derivatives of *S. cerevisiae* SK1 diploids,
454 MSY832/833 (*MATα/MAT**a**, lys2/", ura3/", leu2::hisG/", trp1::hisG/"*). The
455 genotypes of each strain used in this study are described in Supplementary Table
456 S1
457
458 **Strain Construction**
459 The *RFA1-AID* gene was constructed by one-step DNA integration. The AID-

460 9Myc tag was added to the C-terminus of the *RFA1* open reading frame by the
461 transformation of yeast cells (MSY823) with a DNA fragment amplified by PCR
462 using p7AID-9myc (provided by Dr. Neil Hunter) as a template and a pair of
463 primers (Rfa1-AID-Hygoro-F and -R in Supplementary Table S2). The
464 transformants were selected against hygromycin. Genomic DNAs from the
465 candidate colonies were purified and the genomic DNAs were checked for the
466 correct tagging by PCR and DNA sequencing using the primer described in
467 Supplementary Table S2.
468
469 **Anti-serum and antibodies**
470 Anti-myc (9E10, sc-40, Santa Cruz), anti-tubulin (MCA77G, Bio-Rad/Serotec,
471 Ltd), anti-Cdc5 (sc-33625, Santa Cruz), and histone H3 phospho-T11 (ab5168,
472 Abcam) were used for western blotting. Rabbit anti-Rad51 [21] and guinea pig anti-
473 Rad51 [73], rabbit anti-Hop1 [74] and rabbit anti-Rfa2 [75] were home-made and used
474 for staining. Rabbit anti-Ndt80 was a gift by M. Lichten. The secondary antibodies
475 for immuno-staining were Alexa Fluor 488 (Goat, A-21206, Thermo Fisher
476 Scientific) and 594 (Goat, A-211012, Thermo Fisher Scientific) IgG used at a
477 1/2000 dilution. For western blotting, alkaline phosphatase-conjugated secondary
478 antibodies (Promega) were used.
479
480 **Meiotic Time course**
481 *Saccharomyces cerevisiae* SK1 strains were patched onto YPG plates (2%
482 bacteriological peptone, 1% yeast extract, 3% glycerol, 2% bacteriological agar)
483 and incubated at 30 °C for 12 h. Cells were inoculated onto YPD plates (2%
484 bacteriological peptone, 1% yeast extract, 2% glucose, 2% bacteriological agar)
485 and grown for two days to obtain isolated colonies. A single colony was inoculated
486 into 3 ml of YPD liquid medium and grown to saturation at 30 °C overnight. To
487 synchronize cell cultures, the overnight cultures were transferred to pre-warmed
488 SPS medium (1% potassium acetate, 1% bacteriological peptone, 0.5% yeast
489 extract, 0.17% yeast nitrogen base with ammonium sulfate and without amino
490 acids, 0.5% ammonium sulfate, 0.05 M potassium biphthalate) and grown for 16–
491 17 h. Meiosis was induced by transferring the SPS-cultured cells to pre-warmed
492 SPM (1% potassium acetate, 0.02% raffinose). The SPM-cultured cells were
493 harvested at various times after transfer. For Rfa1 depletion from 4 h, $CuSO_4$ was
494 added to 50 mM at 3.5 h. Auxin (3-indoleacetic acid) solved in dimethyl sulfoxide
495 (DMSO) was added at a final concentration of 2 mM at 4 h. In the control

496 experiment (without auxin), we added an equivalent DMSO solution alone.
497
498 **Cytology**
499 Chromosome spreads were immunostained as described previously [48,73].
500 Spheroplasts were burst in the presence of 1% paraformaldehyde and 0.1% lipsol.
501 The spreads were stained with primary and secondary antibodies observed using
502 a fluorescence microscope (BX51; Olympus/Evident) with a 100× objective
503 (NA1.3). Images were captured by CCD camera (CoolSNAP; Roper), and then
504 processed using IP lab and/or iVision (Bio Vision Technologies) and Photoshop
505 (version, 25.4.0; Adobe; https://www.adobe.com) software. For focus counting,
506 ~30 nuclei were counted at each time point.
507 Whole-cell staining was carried out as follows. Yeast cells are fixed with
508 formaldehyde (a final concentration of 3.7%) and collected. The pellets were
509 suspended in the ZK buffer (25 mM Tris-HCl [pH 7.5], 80 mM KCl) and treated
510 with DTT (20 mM) and then with Zymolyase 100T (2.5 μg/mL). After washing with
511 PBS, the cells were placed on a glass slide coated with poly-lysine (1 mg/ml).
512 The cells were treated with cold ethanol (100% 6 min) and acetone (100% 0.5
513 min), and washed with PBS. After blocking with PBS with 1% BSA, cells were
514 stained with primary and secondary antibodies.
515
516 **Western blotting**
517 Western blotting was performed as described previously [22,76] , using cell lysates
518 extracted by the TCA method. After being harvested and washed twice with 20%
519 TCA, cells were roughly disrupted with zirconia beads by the Multi-beads shocker
520 (Yasui Kikai). The protein precipitate recovered by centrifugation was suspended
521 in SDS-PAGE sample buffer adjusted to pH 8.8 and then incubated at 95 °C for
522 10 min. After electrophoresis, the proteins were transferred onto a nylon
523 membrane (Immobilon-P, Millipore) and incubated with primary antibodies in a
524 blocking buffer (1× PBS, 0.5% BSA) and then with alkaline phosphatase-
525 conjugated secondary antibody (Promega). The color reaction was developed
526 with NBT/BCIP solution (Nacalai Tesque).
527
528 **CHEF analysis Pulsed-field gel electrophoresis**
529 For pulsed-field gel electrophoresis (PFGE), chromosomal DNA was prepared in
530 1.3% of low-melting point agarose plugs as described in [74] and run at 14 °C with
531 1X TBE buffer in a CHEF DR-III apparatus (BioRad) using the field 6V/cm at a

532 120° angle for 48 h. Switching times followed a ramp from 15.1 to 25.1 seconds.
533 After the electrophoresis, the gel was stained with 0.5 μg/mL ethidium bromide
534 for 30 min and washed with distilled water. Images were taken using ImageQuant
535 LAS4000 BioImager (GE Healthcare).
536
537 **FACS analysis**
538 Cells in 1 ml of SPM culture were collected by centrifugation. The pellet was then
539 resuspended in 1 ml of 70% ethanol. Fixed cells were recollected and washed by
540 suspending 1 ml of 50 mM sodium citrate buffer. The collected cells were
541 resuspended in 0.5 ml of sodium citrate buffer and sonicated for the 20s at room
542 temperature. Sonicated cells were incubated with 12.5 μl of 10 mg/mL RNAseA
543 for 1 h at 50 °C and in 25 μl of 15mg/ml proteinase K for 1h at 50 °C. 0.5ml of 16
544 μlg/mL PI solution was added and incubated for 30 min at room temperature in
545 the dark. The samples were then analyzed using SA-3800 Spectral analyzer
546 (Sony). Floreada.io was used for gating and plotting graphs.
547
548 **Data availability**
549 Uncropped western blotting images are provided in Supplementary Figures. The
550 raw data used in plots and graphs are also shown in Source Data. The raw
551 microscopy images used for figures and quantification are available from
552 corresponding authors upon request.
553
554 **Acknowledgments**
555 We are grateful to Drs. Neil Hunter for providing the yeast AID system and
556 Michael Lichten for anti-Ndt80. A.Sa. is a JICA fellow. Y.F. and M.I. were
557 supported by the Institute for Protein Research. This work was supported by a
558 grant from Institute for Fermentation, Osaka (IFO) and from Uehara Memorial
559 Foundation to Life Sciences; to A.Sh.
560
561 **Competing interest**
562 The authors declare no competing financial interest.
563
564 **Author contributions**
565 A.Sh. conceived and designed the experiments. A.Sa., Z.C., and Y.T. carried out
566 experiments with help from Y.F. and M.I.. A.Sa, Z.C., Y.T., Y.F., M.I., and A.Sh.
567 analyzed the data. A.Sh. wrote the manuscript with inputs from help from others.

568

569 **References**

570 1 Bhat, K. P. & Cortez, D. RPA and RAD51: fork reversal, fork protection,
571 and genome stability. *Nat Struct Mol Biol* **25**, 446-453 (2018).
572 https://doi.org:10.1038/s41594-018-0075-z

573 2 Caldwell, C. C. & Spies, M. Dynamic elements of replication protein A at
574 the crossroads of DNA replication, recombination, and repair. *Crit Rev*
575 *Biochem Mol Biol* **55**, 482-507 (2020).
576 https://doi.org:10.1080/10409238.2020.1813070

577 3 Wold, M. S. Replication protein A: a heterotrimeric, single-stranded DNA-
578 binding protein required for eukaryotic DNA metabolism. *Annu Rev*
579 *Biochem* **66**, 61-92 (1997).
580 https://doi.org:10.1146/annurev.biochem.66.1.61

581 4 Brill, S. J. & Stillman, B. Replication factor-A from Saccharomyces
582 cerevisiae is encoded by three essential genes coordinately expressed at
583 S phase. *Genes Dev* **5**, 1589-1600 (1991).
584 https://doi.org:10.1101/gad.5.9.1589

585 5 Zou, L. & Elledge, S. J. Sensing DNA damage through ATRIP recognition
586 of RPA-ssDNA complexes. *Science* **300**, 1542-1548 (2003).
587 https://doi.org:10.1126/science.1083430

588 6 Chen, H., Lisby, M. & Symington, L. S. RPA coordinates DNA end resection
589 and prevents formation of DNA hairpins. *Mol Cell* **50**, 589-600 (2013).
590 https://doi.org:10.1016/j.molcel.2013.04.032

591 7 Sasanuma, H. *et al.* A new protein complex promoting the assembly of
592 Rad51 filaments. *Nat Commun* **4**, 1676 (2013).
593 https://doi.org:10.1038/ncomms2678

594 8 Shinohara, A. & Ogawa, T. Stimulation by Rad52 of yeast Rad51-mediated
595 recombination. *Nature* **391**, 404-407 (1998). https://doi.org:10.1038/34943

596 9 Sung, P. Yeast Rad55 and Rad57 proteins form a heterodimer that
597 functions with replication protein A to promote DNA strand exchange by
598 Rad51 recombinase. *Genes Dev* **11**, 1111-1121 (1997).
599 https://doi.org:10.1101/gad.11.9.1111

600 10 Sung, P. Catalysis of ATP-dependent homologous DNA pairing and strand
601 exchange by yeast RAD51 protein. *Science* **265**, 1241-1243 (1994).
602 https://doi.org:10.1126/science.8066464

603 11 Friedel, A. M., Pike, B. L. & Gasser, S. M. ATR/Mec1: coordinating fork

604 stability and repair. *Curr Opin Cell Biol* **21**, 237-244 (2009).
605 https://doi.org:10.1016/j.ceb.2009.01.017
606 12 Williams, R. M., Yates, L. A. & Zhang, X. Structures and regulations of ATM
607 and ATR, master kinases in genome integrity. *Curr Opin Struct Biol* **61**, 98-
608 105 (2020). https://doi.org:10.1016/j.sbi.2019.12.010
609 13 Biswas, H., Goto, G., Wang, W., Sung, P. & Sugimoto, K. Ddc2ATRIP
610 promotes Mec1ATR activation at RPA-ssDNA tracts. *PLoS Genet* **15**,
611 e1008294 (2019). https://doi.org:10.1371/journal.pgen.1008294
612 14 Deshpande, I. *et al.* Structural Basis of Mec1-Ddc2-RPA Assembly and
613 Activation on Single-Stranded DNA at Sites of Damage. *Mol Cell* **68**, 431-
614 445 e435 (2017). https://doi.org:10.1016/j.molcel.2017.09.019
615 15 Yates, L. A., Tannous, E. A., Morgan, R. M., Burgers, P. M. & Zhang, X. A
616 DNA damage-induced phosphorylation circuit enhances Mec1(ATR)
617 Ddc2(ATRIP) recruitment to Replication Protein A. *Proceedings of the*
618 *National Academy of Sciences of the United States of America* **120**,
619 e2300150120 (2023). https://doi.org:10.1073/pnas.2300150120
620 16 Bass, T. E. *et al.* ETAA1 acts at stalled replication forks to maintain genome
621 integrity. *Nat Cell Biol* **18**, 1185-1195 (2016).
622 https://doi.org:10.1038/ncb3415
623 17 Haahr, P. *et al.* Activation of the ATR kinase by the RPA-binding protein
624 ETAA1. *Nat Cell Biol* **18**, 1196-1207 (2016).
625 https://doi.org:10.1038/ncb3422
626 18 Bergerat, A. *et al.* An atypical topoisomerase II from Archaea with
627 implications for meiotic recombination. *Nature* **386**, 414-417 (1997).
628 https://doi.org:10.1038/386414a0
629 19 Keeney, S., Giroux, C. N. & Kleckner, N. Meiosis-specific DNA double-
630 strand breaks are catalyzed by Spo11, a member of a widely conserved
631 protein family. *Cell* **88**, 375-384 (1997).
632 20 Bishop, D. K., Park, D., Xu, L. & Kleckner, N. DMC1: a meiosis-specific
633 yeast homolog of E. coli recA required for recombination, synaptonemal
634 complex formation, and cell cycle progression. *Cell* **69**, 439-456 (1992).
635 21 Shinohara, A., Ogawa, H. & Ogawa, T. Rad51 protein involved in repair
636 and recombination in S. cerevisiae is a RecA-like protein. *Cell* **69**, 457-470
637 (1992).
638 22 Hayase, A. *et al.* A protein complex containing Mei5 and Sae3 promotes
639 the assembly of the meiosis-specific RecA homolog Dmc1. *Cell* **119**, 927-

940 (2004).

23 Tsubouchi, H. & Roeder, G. S. The budding yeast mei5 and sae3 proteins act together with dmc1 during meiotic recombination. *Genetics* **168**, 1219-1230 (2004). https://doi.org:10.1534/genetics.103.025700

24 Hong, S. *et al.* The logic and mechanism of homologous recombination partner choice. *Mol Cell* **51**, 440-453 (2013). https://doi.org:10.1016/j.molcel.2013.08.008

25 Kim, K. P. *et al.* Sister cohesion and structural axis components mediate homolog bias of meiotic recombination. *Cell* **143**, 924-937 (2010). https://doi.org:10.1016/j.cell.2010.11.015

26 Niu, H. *et al.* Partner choice during meiosis is regulated by Hop1-promoted dimerization of Mek1. *Molecular biology of the cell* **16**, 5804-5818 (2005). https://doi.org:10.1091/mbc.e05-05-0465

27 Leem, S. H. & Ogawa, H. The MRE4 gene encodes a novel protein kinase homologue required for meiotic recombination in Saccharomyces cerevisiae. *Nucleic Acids Res* **20**, 449-457 (1992). https://doi.org:10.1093/nar/20.3.449

28 Rockmill, B. & Roeder, G. S. A meiosis-specific protein kinase homolog required for chromosome synapsis and recombination. *Genes Dev* **5**, 2392-2404 (1991). https://doi.org:10.1101/gad.5.12b.2392

29 Callender, T. L. *et al.* Mek1 Down Regulates Rad51 Activity during Yeast Meiosis by Phosphorylation of Hed1. *PLoS Genet* **12**, e1006226 (2016). https://doi.org:10.1371/journal.pgen.1006226

30 Niu, H. *et al.* Regulation of meiotic recombination via Mek1-mediated Rad54 phosphorylation. *Mol Cell* **36**, 393-404 (2009). https://doi.org:10.1016/j.molcel.2009.09.029

31 Shinohara, M. *et al.* Characterization of the roles of the Saccharomyces cerevisiae RAD54 gene and a homologue of RAD54, RDH54/TID1, in mitosis and meiosis. *Genetics* **147**, 1545-1556 (1997). https://doi.org:10.1093/genetics/147.4.1545

32 Tsubouchi, H. & Roeder, G. S. Budding yeast Hed1 down-regulates the mitotic recombination machinery when meiotic recombination is impaired. *Genes Dev* **20**, 1766-1775 (2006). https://doi.org:10.1101/gad.1422506

33 Borner, G. V., Hochwagen, A. & MacQueen, A. J. Meiosis in budding yeast. *Genetics* (2023). https://doi.org:10.1093/genetics/iyad125

34 Cartagena-Lirola, H., Guerini, I., Manfrini, N., Lucchini, G. & Longhese, M.

676 P. Role of the Saccharomyces cerevisiae Rad53 checkpoint kinase in
677 signaling double-strand breaks during the meiotic cell cycle. *Molecular and*
678 *cellular biology* **28**, 4480-4493 (2008).
679 https://doi.org:10.1128/MCB.00375-08
680 35 Usui, T. & Shinohara, A. Rad9, a 53BP1 Ortholog of Budding Yeast, Is
681 Insensitive to Spo11-Induced Double-Strand Breaks During Meiosis. *Front*
682 *Cell Dev Biol* **9**, 635383 (2021). https://doi.org:10.3389/fcell.2021.635383
683 36 Carballo, J. A., Johnson, A. L., Sedgwick, S. G. & Cha, R. S.
684 Phosphorylation of the axial element protein Hop1 by Mec1/Tel1 ensures
685 meiotic interhomolog recombination. *Cell* **132**, 758-770 (2008).
686 https://doi.org:10.1016/j.cell.2008.01.035
687 37 Hollingsworth, N. M. Mek1/Mre4 is a master regulator of meiotic
688 recombination in budding yeast. *Microb Cell* **3**, 129-131 (2016).
689 https://doi.org:10.15698/mic2016.03.487
690 38 Chen, X. *et al.* Mek1 coordinates meiotic progression with DNA break
691 repair by directly phosphorylating and inhibiting the yeast pachytene exit
692 regulator Ndt80. *PLoS Genet* **14**, e1007832 (2018).
693 https://doi.org:10.1371/journal.pgen.1007832
694 39 Hochwagen, A. Meiosis: making a synaptonemal complex just got easier.
695 *Curr Biol* **19**, R849-851 (2009). https://doi.org:10.1016/j.cub.2009.07.001
696 40 Sourirajan, A. & Lichten, M. Polo-like kinase Cdc5 drives exit from
697 pachytene during budding yeast meiosis. *Genes Dev* **22**, 2627-2632
698 (2008). https://doi.org:10.1101/gad.1711408
699 41 Sym, M., Engebrecht, J. A. & Roeder, G. S. ZIP1 is a synaptonemal
700 complex protein required for meiotic chromosome synapsis. *Cell* **72**, 365-
701 378 (1993).
702 42 Huang, Y. & Roig, I. Genetic control of meiosis surveillance mechanisms
703 in mammals. *Front Cell Dev Biol* **11**, 1127440 (2023).
704 https://doi.org:10.3389/fcell.2023.1127440
705 43 MacQueen, A. J. & Hochwagen, A. Checkpoint mechanisms: the puppet
706 masters of meiotic prophase. *Trends Cell Biol* **21**, 393-400 (2011).
707 https://doi.org:10.1016/j.tcb.2011.03.004
708 44 Borner, G. V., Kleckner, N. & Hunter, N. Crossover/noncrossover
709 differentiation, synaptonemal complex formation, and regulatory
710 surveillance at the leptotene/zygotene transition of meiosis. *Cell* **117**, 29-
711 45 (2004).

45 Storlazzi, A., Xu, L., Schwacha, A. & Kleckner, N. Synaptonemal complex (SC) component Zip1 plays a role in meiotic recombination independent of SC polymerization along the chromosomes. *Proceedings of the National Academy of Sciences of the United States of America* **93**, 9043-9048 (1996). https://doi.org:10.1073/pnas.93.17.9043

46 Grushcow, J. M. *et al.* Saccharomyces cerevisiae checkpoint genes MEC1, RAD17 and RAD24 are required for normal meiotic recombination partner choice. *Genetics* **153**, 607-620 (1999). https://doi.org:10.1093/genetics/153.2.607

47 Shinohara, M., Hayashihara, K., Grubb, J. T., Bishop, D. K. & Shinohara, A. DNA damage response clamp 9-1-1 promotes assembly of ZMM proteins for formation of crossovers and synaptonemal complex. *Journal of cell science* **128**, 1494-1506 (2015). https://doi.org:10.1242/jcs.161554

48 Shinohara, M., Sakai, K., Ogawa, T. & Shinohara, A. The mitotic DNA damage checkpoint proteins Rad17 and Rad24 are required for repair of double-strand breaks during meiosis in yeast. *Genetics* **164**, 855-865 (2003). https://doi.org:10.1093/genetics/164.3.855

49 Kim, H. S. & Brill, S. J. Rfc4 interacts with Rpa1 and is required for both DNA replication and DNA damage checkpoints in Saccharomyces cerevisiae. *Molecular and cellular biology* **21**, 3725-3737 (2001). https://doi.org:10.1128/MCB.21.11.3725-3737.2001

50 Refolio, E., Cavero, S., Marcon, E., Freire, R. & San-Segundo, P. A. The Ddc2/ATRIP checkpoint protein monitors meiotic recombination intermediates. *Journal of cell science* **124**, 2488-2500 (2011). https://doi.org:10.1242/jcs.081711

51 Joo, J. H. *et al.* RPA interacts with Rad52 to promote meiotic crossover and noncrossover recombination. *Nucleic Acids Res* (2024). https://doi.org:10.1093/nar/gkae083

52 Shi, B. *et al.* Dual functions for the ssDNA-binding protein RPA in meiotic recombination. *PLoS Genet* **15**, e1007952 (2019). https://doi.org:10.1371/journal.pgen.1007952

53 Nishimura, K., Fukagawa, T., Takisawa, H., Kakimoto, T. & Kanemaki, M. An auxin-based degron system for the rapid depletion of proteins in nonplant cells. *Nat Methods* **6**, 917-922 (2009). https://doi.org:10.1038/nmeth.1401

54 Gasior, S. L., Wong, A. K., Kora, Y., Shinohara, A. & Bishop, D. K. Rad52

748 associates with RPA and functions with rad55 and rad57 to assemble
749 meiotic recombination complexes. *Genes Dev* **12**, 2208-2221 (1998).
750 https://doi.org:10.1101/gad.12.14.2208
751 55 Chu, S. *et al.* The transcriptional program of sporulation in budding yeast.
752 *Science* **282**, 699-705 (1998).
753 https://doi.org:10.1126/science.282.5389.699
754 56 Bishop, D. K. RecA homologs Dmc1 and Rad51 interact to form multiple
755 nuclear complexes prior to meiotic chromosome synapsis. *Cell* **79**, 1081-
756 1092 (1994).
757 57 Hollingsworth, N. M., Goetsch, L. & Byers, B. The HOP1 gene encodes a
758 meiosis-specific component of yeast chromosomes. *Cell* **61**, 73-84 (1990).
759 https://doi.org:10.1016/0092-8674(90)90216-2
760 58 Smith, A. V. & Roeder, G. S. The yeast Red1 protein localizes to the cores
761 of meiotic chromosomes. *J Cell Biol* **136**, 957-967 (1997).
762 https://doi.org:10.1083/jcb.136.5.957
763 59 Kniewel, R. *et al.* Histone H3 Threonine 11 Phosphorylation Is Catalyzed
764 Directly by the Meiosis-Specific Kinase Mek1 and Provides a Molecular
765 Readout of Mek1 Activity in Vivo. *Genetics* **207**, 1313-1333 (2017).
766 https://doi.org:10.1534/genetics.117.300359
767 60 Shinohara, A., Gasior, S., Ogawa, T., Kleckner, N. & Bishop, D. K.
768 Saccharomyces cerevisiae recA homologues RAD51 and DMC1 have
769 both distinct and overlapping roles in meiotic recombination. *Genes Cells*
770 **2**, 615-629 (1997). https://doi.org:10.1046/j.1365-2443.1997.1480347.x
771 61 Raina, V. B. & Vader, G. Homeostatic Control of Meiotic Prophase
772 Checkpoint Function by Pch2 and Hop1. *Curr Biol* **30**, 4413-4424 e4415
773 (2020). https://doi.org:10.1016/j.cub.2020.08.064
774 62 Hollingsworth, N. M. & Gaglione, R. The meiotic-specific Mek1 kinase in
775 budding yeast regulates interhomolog recombination and coordinates
776 meiotic progression with double-strand break repair. *Curr Genet* **65**, 631-
777 641 (2019). https://doi.org:10.1007/s00294-019-00937-3
778 63 Alani, E., Padmore, R. & Kleckner, N. Analysis of wild-type and rad50
779 mutants of yeast suggests an intimate relationship between meiotic
780 chromosome synapsis and recombination. *Cell* **61**, 419-436 (1990).
781 https://doi.org:10.1016/0092-8674(90)90524-i
782 64 Usui, T., Ogawa, H. & Petrini, J. H. A DNA damage response pathway
783 controlled by Tel1 and the Mre11 complex. *Mol Cell* **7**, 1255-1266 (2001).

784 https://doi.org:10.1016/s1097-2765(01)00270-2
785 65 Lin, Y. *et al.* APE1 recruits ATRIP to ssDNA in an RPA-dependent and -
786 independent manner to promote the ATR DNA damage response. *Elife* **12**
787 (2023). https://doi.org:10.7554/eLife.82324
788 66 Shinohara, M., Bishop, D. K. & Shinohara, A. Distinct Functions in
789 Regulation of Meiotic Crossovers for DNA Damage Response Clamp
790 Loader Rad24(Rad17) and Mec1(ATR) Kinase. *Genetics* **213**, 1255-1269
791 (2019). https://doi.org:10.1534/genetics.119.302427
792 67 San-Segundo, P. A. & Roeder, G. S. Pch2 links chromatin silencing to
793 meiotic checkpoint control. *Cell* **97**, 313-324 (1999).
794 https://doi.org:10.1016/s0092-8674(00)80741-2
795 68 Borner, G. V., Barot, A. & Kleckner, N. Yeast Pch2 promotes domainal axis
796 organization, timely recombination progression, and arrest of defective
797 recombinosomes during meiosis. *Proceedings of the National Academy of*
798 *Sciences of the United States of America* **105**, 3327-3332 (2008).
799 https://doi.org:10.1073/pnas.0711864105
800 69 Herruzo, E. *et al.* The Pch2 AAA+ ATPase promotes phosphorylation of
801 the Hop1 meiotic checkpoint adaptor in response to synaptonemal
802 complex defects. *Nucleic Acids Res* **44**, 7722-7741 (2016).
803 https://doi.org:10.1093/nar/gkw506
804 70 Humphryes, N. *et al.* The Ecm11-Gmc2 complex promotes synaptonemal
805 complex formation through assembly of transverse filaments in budding
806 yeast. *PLoS Genet* **9**, e1003194 (2013).
807 https://doi.org:10.1371/journal.pgen.1003194
808 71 Lee, M. S. *et al.* The synaptonemal complex central region modulates
809 crossover pathways and feedback control of meiotic double-strand break
810 formation. *Nucleic Acids Res* **49**, 7537-7553 (2021).
811 https://doi.org:10.1093/nar/gkab566
812 72 Gonzalez-Arranz, S. *et al.* Functional Impact of the H2A.Z Histone Variant
813 During Meiosis in Saccharomyces cerevisiae. *Genetics* **209**, 997-1015
814 (2018). https://doi.org:10.1534/genetics.118.301110
815 73 Shinohara, M., Gasior, S. L., Bishop, D. K. & Shinohara, A. Tid1/Rdh54
816 promotes colocalization of rad51 and dmc1 during meiotic recombination.
817 *Proceedings of the National Academy of Sciences of the United States of*
818 *America* **97**, 10814-10819 (2000).
819 https://doi.org:10.1073/pnas.97.20.10814

74 Bani Ismail, M., Shinohara, M. & Shinohara, A. Dot1-dependent histone H3K79 methylation promotes the formation of meiotic double-strand breaks in the absence of histone H3K4 methylation in budding yeast. *PLoS One* **9**, e96648 (2014). https://doi.org:10.1371/journal.pone.0096648

75 Sasanuma, H., Furihata, Y., Shinohara, M. & Shinohara, A. Remodeling of the Rad51 DNA strand-exchange protein by the Srs2 helicase. *Genetics* **194**, 859-872 (2013). https://doi.org:10.1534/genetics.113.150615

76 Shinohara, M., Oh, S. D., Hunter, N. & Shinohara, A. Crossover assurance and crossover interference are distinctly regulated by the ZMM proteins during yeast meiosis. *Nat Genet* **40**, 299-309 (2008). https://doi.org:10.1038/ng.83

833

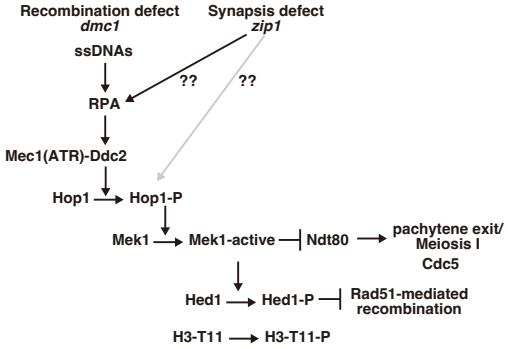

834

835 **Figure 1. A pathway of recombination checkpoint in meiosis.**

836

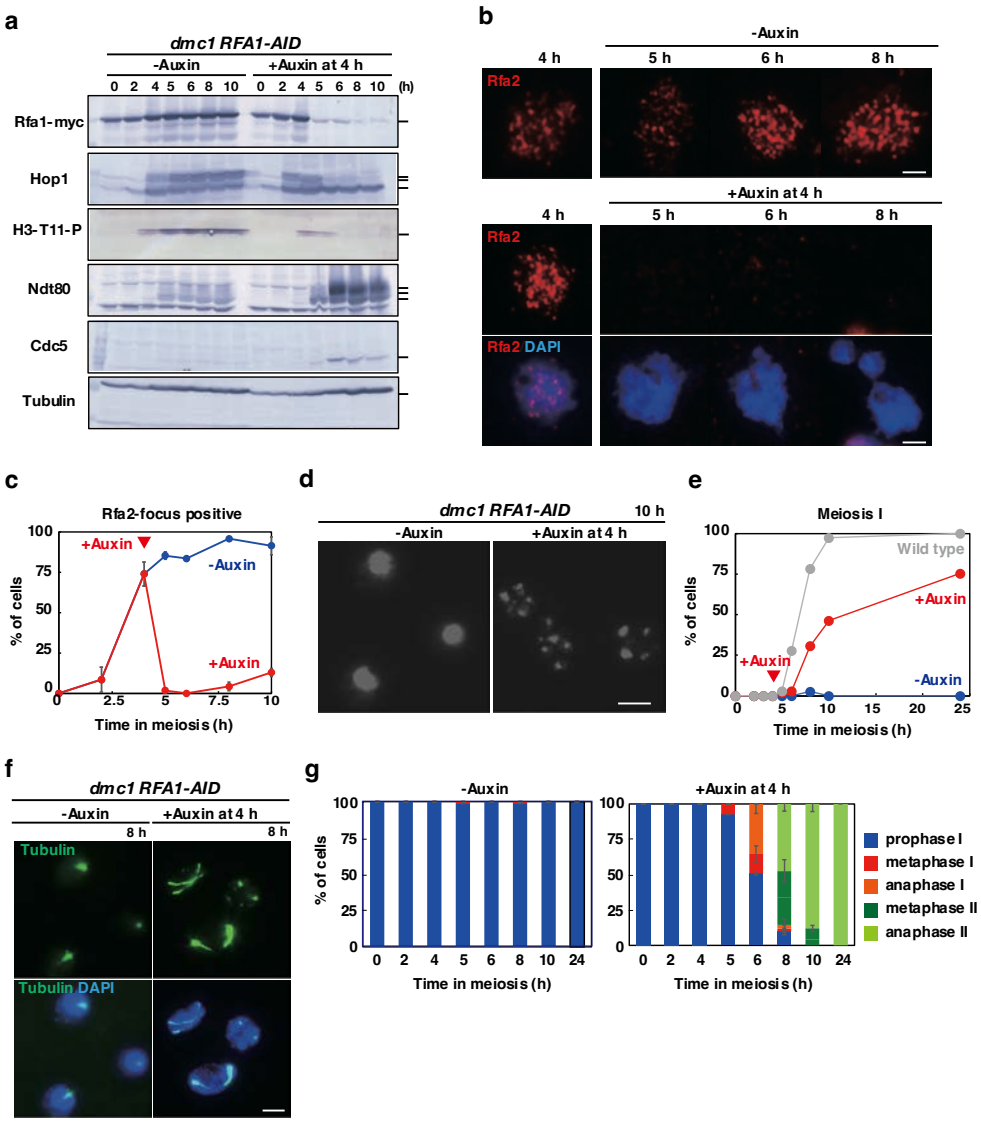

Figure 2. Rfa1 depletion alleviates *dmc1*-induced pachytene arrest

(a) Expression of various proteins in meiosis. Lysates obtained from the *dmc1 RFA1-AID* (SAY63/64) cells at various time points during meiosis with the addition of auxin (2 mM) in DMSO or DMSO alone at 4 h were analyzed by western blotting using anti-myc (Rfa1-myc-AID, upper), anti-Hop1, anti-histone H3-phospho-T11, anti-Ndt80, anti-Cdc5 or anti-tubulin (lower) antibodies.

(b) Rfa2 staining. Nuclear spreads from *dmc1 RFA1-AID* (SAY63/64) cells with or without the addition of auxin at 4 h were stained with anti-Rfa2 (red), and DAPI (blue). Representative images at each time point under the two conditions are shown. Bar = 2 μm.

849 (c) Kinetics of Rfa2 assembly/disassembly. The number of Rfa2-positive cells
850 (with more than 5 foci) was counted at each time point. At each time point,
851 more than 100 cells were counted.
852 (d) Meiosis progression. *dmc1 RFA1-AID* (SAY63/64) cells were analyzed by
853 DAPI staining. Representative image of cells treated with/without 4 h-auxin
854 addition at 10 h are shown. Bar = 2 μm.
855 (e) Meiosis progression. The entry into meiosis I and II in *dmc1 RFA1-AID*
856 (SAY63/64) cells were analyzed by DAPI staining. The number of DAPI
857 bodies in a cell was counted. A cell with 2, 3, and 4, and 3 and 4 DAPI bodies
858 was defined as a cell that passed through meiosis I and meiosis II,
859 respectively. The graph shows the percentages of cells that completed MI or
860 MII at the indicated time points. More than 200 cells were counted at each
861 time point. The representative results (*n*=3) are shown. *dmc1 RFA1-AID*
862 without auxin (with DMSO), blue closed circles; *dmc1 RFA1-AID* with auxin
863 addition at 4 h, red closed circles; Wild type (MSY823/833), gray circles.
864 (f) Whole cells were fixed and stained with anti-tubulin (green) and DAPI (blue).
865 Representative images at 8 h of *dmc1 RFA1-AID* (SAY63/64) cells with or
866 without the addition of auxin at 4 h are shown. Bar = 2 μm.
867 (g) Classification of tubulin staining at each time point of meiosis in *dmc1 RFA1-*
868 *AID* (SAY63/64) cells with (right) or without (left) the addition of auxin at 4 h.
869 Dot, short line, and long line tubulin-staining with single DAPI mass were
870 defined as prophase I (blue), metaphase I (red), anaphase I (orange),
871 metaphase II (green) and anaphase II (light green). At each time point, more
872 than 100 cells were counted. The representative results are shown (*n*=3).
873

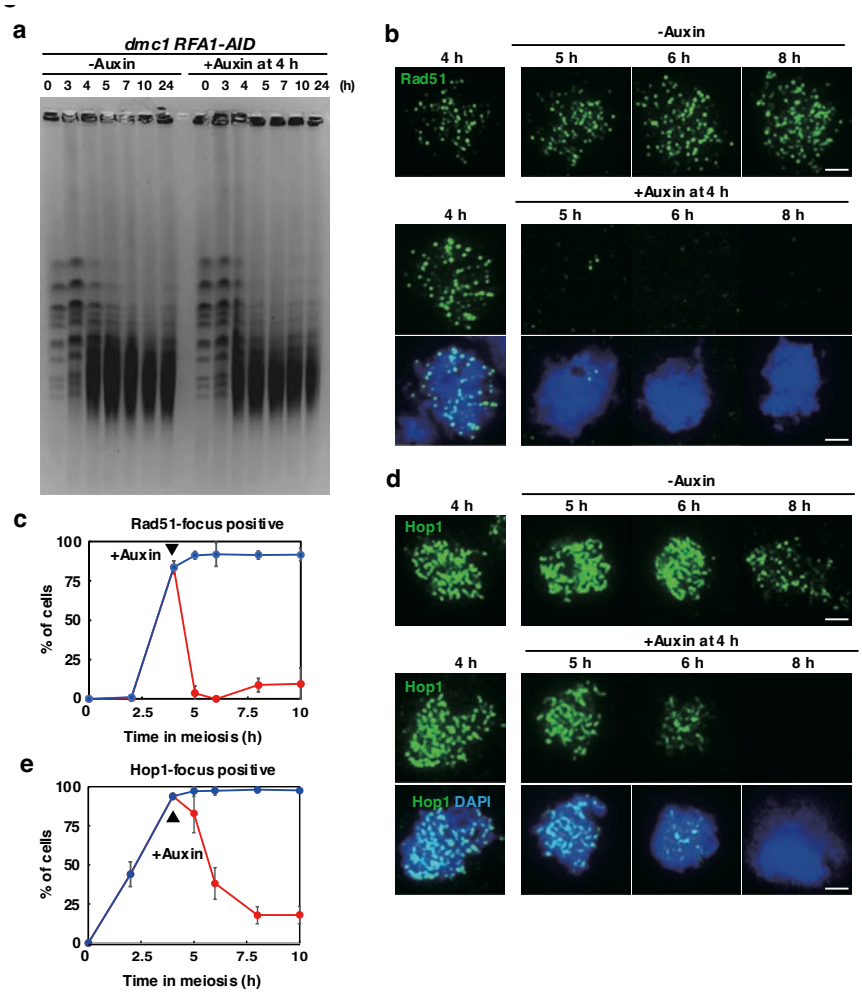

874
875 **Figure 3. Rfa1 depletion does not affect DSB turnover in *dmc1* mutant**
876 (a) CHEF analysis of meiotic DSB repair. Chromosomal DNAs from *dmc1 RFA1-*
877 *AID* (SAY63/64) cells with the addition of auxin (2 mM) in DMSO or DMSO
878 alone at 4 h were studied by CHEF electrophoresis. The gel is stained with
879 EtBr. Auxin was added at 4 h in the incubation with SPM.
880 (b) Rad51 staining. Nuclear spreads from *dmc1 RFA1-AID* (SAY63/64) cells with
881 or without the addition of auxin at 4 h were stained with anti-Rad51 (green),
882 and DAPI (blue). Representative images at each time point under the two
883 conditions are shown. Bar = 2 μm.
884 (c) Kinetics of Rad51 assembly/disassembly. The number of Rad51-positive cells
885 (with more than 5 foci) was counted at each time point. At each time point,
886 more than 100 cells were counted.
887 (d) Hop1 staining. Nuclear spreads from *dmc1 RFA1-AID* (SAY63/64) cells with
888 or without the addition of auxin at 4 h were stained with anti-Hop1 (green),
889 and DAPI (blue). Representative images at each time point under the two

890 conditions are shown. Bar = 2 μm.

891 (e) Kinetics of Hop1 assembly/disassembly. The number of Rad51-positive cells
892 (with more than 5 foci) was counted at each time point. At each time point,
893 more than 100 cells were counted.

894

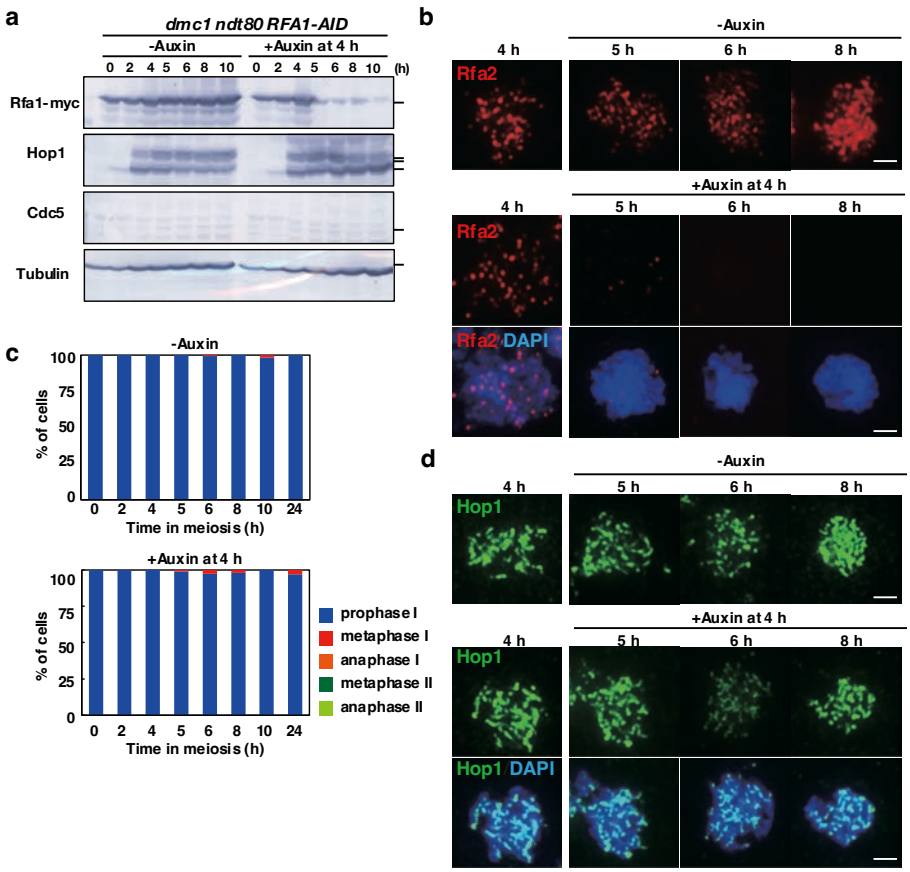

Figure 4. *NDT80* is necessary for pachytene exit by Rfa1 depletion

(a) Expression of various protein in meiosis. Lysates obtained from the *ndt80 dmc1 RFA1-AID* (SAY80/81) cells at various time points during meiosis with the addition of auxin (2 mM) in DMSO or DMSO alone were analyzed by western blotting using anti-myc (Rfa1-myc-AID, upper), anti-Hop1, anti-Cdc5 or anti-tubulin (lower) antibodies.

(b) Rfa2 staining. Nuclear spreads from *ndt80 dmc1 RFA1-AID* (SAY80/81) cells with or without the addition of auxin at 4 h were stained with anti-Rfa2 (red), and DAPI (blue). Representative images at each time point under the two conditions are shown. Bar = 2 μm.

(c) Classification of tubulin staining at each time point of meiosis in *ndt80 dmc1 RFA1-AID* (SAY80/81) cells with (right) or without (left) the addition of auxin at 4 h. Dot, short line, and long line tubulin-staining with single DAPI mass were defined as prophase I (blue), metaphase I (red), anaphase I (orange), metaphase II (blue), anaphase II (green) and post-meiosis II (pale green). Short and long tubulin-staining were defined as metaphase II and anaphase

912 II, respectively. At each time point, more than 100 cells were counted. The
913 representative results are shown (*n*=2).
914 (d) Hop1 staining. Nuclear spreads from *ndt80 dmc1 RFA1-AID* (SAY SAY80/81)
915 cells with or without the addition of auxin at 4 h were stained with anti-Hop1
916 (green), and DAPI (blue). Representative images at each time point under the
917 two conditions are shown. Bar = 2 μm.
918

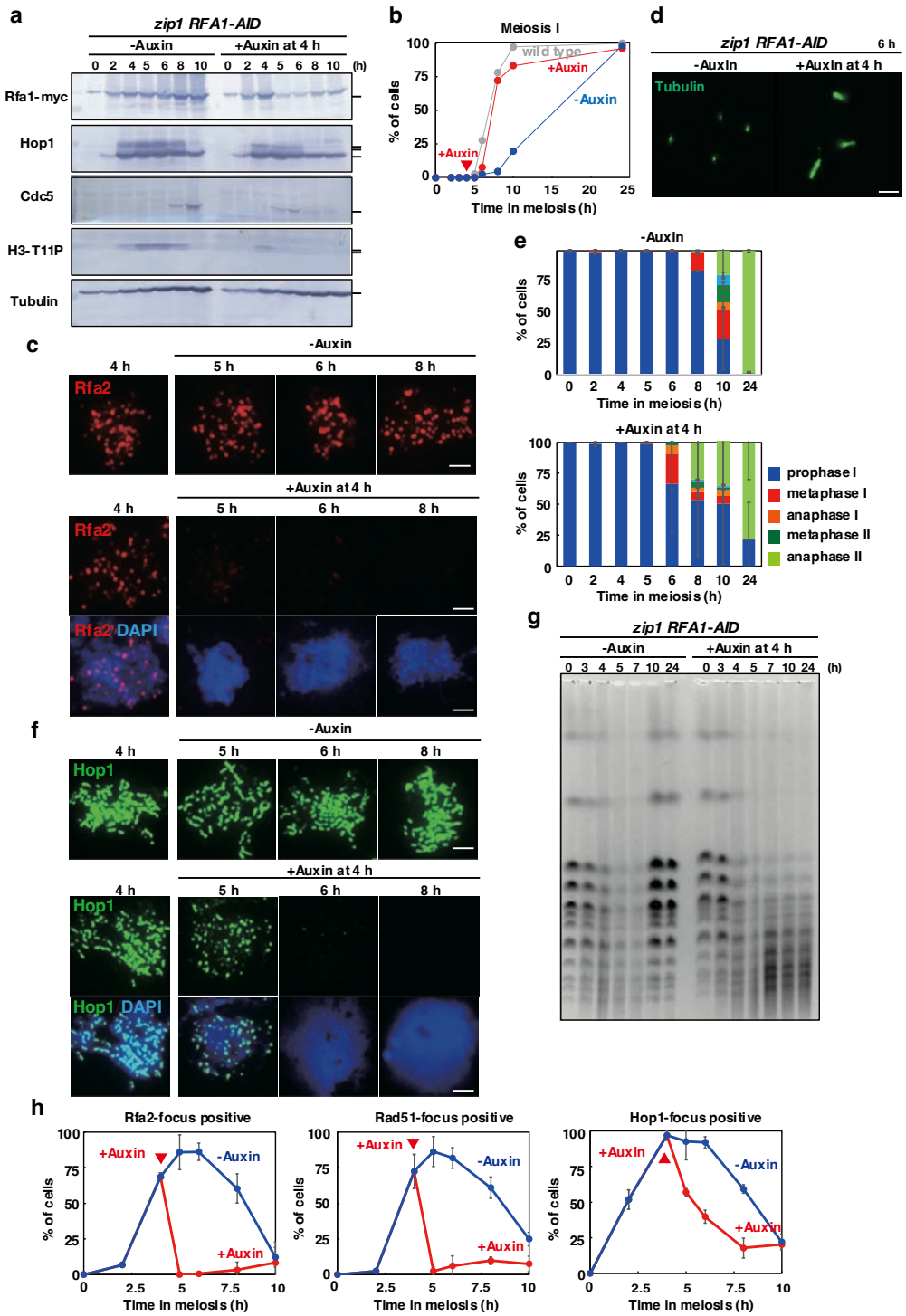

Figure 5. Rfa1 depletion alleviates *zip1*-induced delay in meiosis I

(a) Expression of various proteins in meiosis. Lysates obtained from the *zip1 RFA1-AID* (SAY72/73) cells at various time points during meiosis with the addition of auxin (2 mM) in DMSO or DMSO alone were analyzed by western

924 blotting using anti-myc (Rfa1-myc-AID, upper), anti-Hop1, anti-Cdc5, anti-
925 histone H3-phospho-T11 or anti-tubulin (lower) antibodies.
926 (b) Meiotic cell cycle progression. The entry into meiosis I and II in *zip1 RFA1-*
927 *AID* (SAY72/73) cells were analyzed by DAPI staining as shown in Figure 2D.
928 More than 200 cells were counted at each time point. The representative
929 results (*n*=3) are shown. *dmc1 RFA1-AID* without auxin, blue closed circles;
930 *dmc1 RFA1-AID* with auxin addition at 4 h, red closed circles.
931 (c) Rfa2 staining. Nuclear spreads from *zip1 RFA1-AID* (SAY72/73) cells with or
932 without the addition of auxin at 4 h were stained with anti-Rfa2 (red), and DAPI
933 (blue). Representative images at each time point under the two conditions are
934 shown. Bar = 2 μm.
935 (d) Tubulin staining in the *zip1 RFA1-AID* mutant. Whole cells were fixed and
936 stained with anti-tubulin (green) and DAPI (blue). Representative images for
937 each class are shown. Bar = 2 μm.
938 (e) Classification of tubulin staining at each time point of meiosis in *zip1 RFA1-*
939 *AID* (SAY72/73) cells with (right) or without (left) the addition of auxin at 4 h.
940 The quantification was performed as shown in Figure 1G. At each time point,
941 more than 100 cells were counted. The representative results are shown (*n*=2).
942 (f) Hop1 staining. Nuclear spreads from *zip1 RFA1-AID* (SAY72/73) cells with or
943 without the addition of auxin at 4 h were stained with anti-Hop1 (green), and
944 DAPI (blue). Representative images at each time point under the two
945 conditions are shown. Bar = 2 μm.
946 (g) CHEF analysis of meiotic DSB repair. Chromosomal DNAs from *zip1 RFA1-*
947 *AID* (SAY72/73) cells with or without the addition of auxin at 4 h were studied
948 by CHEF electrophoresis. Auxin was added at 4 h in the incubation with SPM.
949 (h) Kinetics of assembly/disassembly of Rfa2 (left), Rad51 (middle), and Hop1
950 (right). The number of focus-positive cells (with more than 5 foci) was counted
951 for Rfa2 and Rad51 at each time point. At each time point, more than 100
952 cells were counted.
953

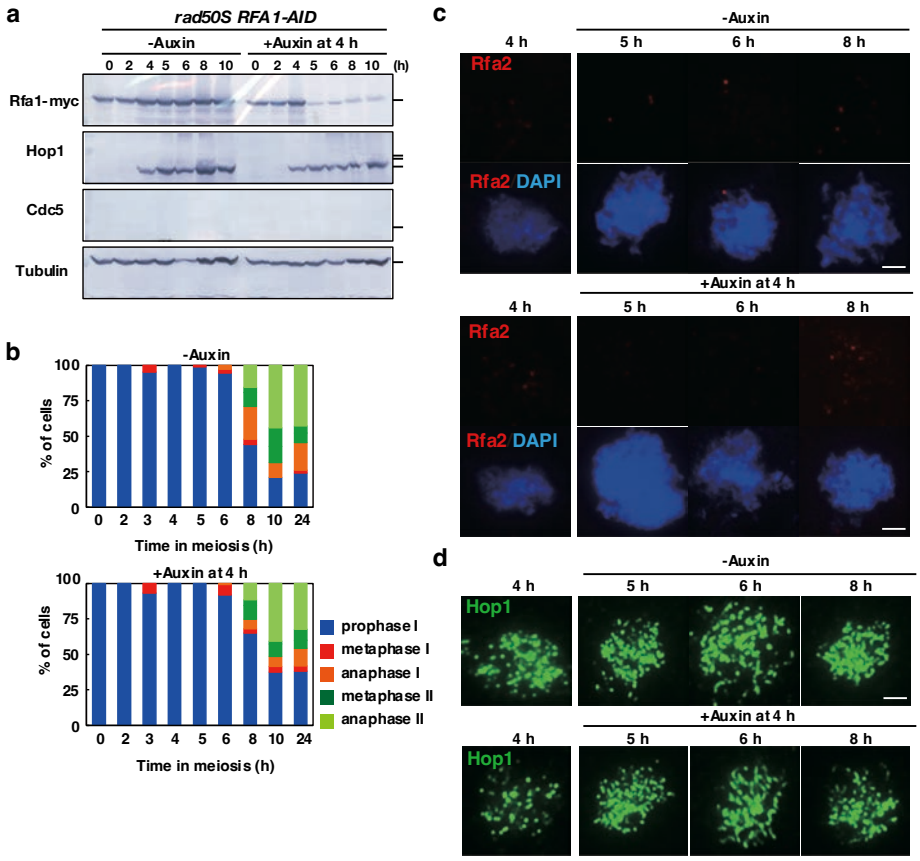

954

955 **Figure 6. Rfa1 depletion does not suppress *rad50S*-induced delay in**
956 **meiosis I**

957 (a) Expression of various proteins in meiosis. Lysates obtained from the *rad50S*
958 *RFA1-AID* (SAY68/69) cells at various time points during meiosis with the
959 addition of auxin (2 mM) in DMSO or DMSO alone were analyzed by western
960 blotting using anti-myc (Rfa1-myc-AID, upper), anti-Hop1, anti-Cdc5 or anti-
961 tubulin (lower) antibodies.

962 (b) Classification of tubulin staining at each time point of meiosis in *rad50S RFA1-*
963 *AID* (SAY68/69) cells with (right) or without (left) the addition of auxin at 4 h.
964 The quantification was performed as shown in Figure 1G. At each time point,
965 more than 100 cells were counted. The representative results are shown (n=1).

966 (c) Rfa2 staining. Nuclear spreads from *rad50S RFA1-AID* (SAY68/69) cells with
967 or without the addition of auxin at 4 h were stained with anti-Rfa2 (red), and
968 DAPI (blue). Representative images at each time point under the two
969 conditions are shown. Bar = 2 μm.

970 (d) Hop1 staining. Nuclear spreads from *rad50S RFA1-AID* (SAY68/69) cells with

971 or without the addition of auxin at 4 h were stained with anti-Hop1 (red), and
972 DAPI (blue). Representative images at each time point under the two
973 conditions are shown. Bar = 2 μm.
974